

# Uteroplacental insufficiency alters rat hippocampal cellular phenotype in conjunction with ErbB receptor expression

Camille Fung<sup>1</sup>, Xingrao Ke<sup>1</sup>, Ashley S. Brown<sup>1</sup>, Xing Yu<sup>1</sup>, Robert A. McKnight<sup>1</sup> and Robert H. Lane<sup>1</sup>

**INTRODUCTION:** Uteroplacental insufficiency (UPI) produces significant neurodevelopmental deficits affecting the hippocampus of intrauterine growth-restricted (IUGR) offspring. IUGR males have worse deficits as compared with IUGR females. The exact mechanisms underlying these deficits are unclear. Alterations in hippocampal cellular composition along with altered expression of neural stem cell (NSC) differentiation molecules may underlie these deficits. We hypothesized that IUGR hippocampi would be endowed with altered neuronal, astrocytic, and immature oligodendrocytic proportions at birth, with males showing greater cellular deficits. We further hypothesized that UPI would perturb rat hippocampal expression of ErbB receptors (ErbB-Rs) and neuregulin 1 (NRG1) at birth and at weaning to account for the short- and long-term IUGR neurological sequelae.

**METHODS:** A well-established rat model of bilateral uterine artery ligation at embryonic day 19.5 was used to induce IUGR.

**RESULTS:** As compared with gender-matched controls, IUGR offspring have altered hippocampal neuronal, astrocytic, and immature oligodendrocytic composition in a subregion- and gender-specific manner at birth. In addition, IUGR hippocampi have altered receptor type- and gender-specific ErbB-R expression at birth and at weaning.

**DISCUSSION:** These cellular and molecular alterations may account for the neurodevelopmental complications of IUGR and for the male susceptibility to worse neurologic outcomes.

Uteroplacental insufficiency (UPI) is the most common cause of intrauterine growth restriction (IUGR) of a fetus in developed countries and leads to short- and long-term neurodevelopmental disabilities in the offspring. These disabilities include tonal abnormalities, difficulties in working memory, recognition memory, visual spatial tasks, behavior, and concentration (1). Correlating with these functional deficits, neuroimaging has shown that hippocampal volume within the cortical gray matter is particularly reduced in human IUGR infants (2). In addition, male IUGR offspring demonstrate an increased severity of neurological impairment as compared with female IUGR offspring (3,4).

The exact mechanisms underlying IUGR-associated neurodevelopmental disabilities are unclear. Furthermore, the male susceptibility to worse neurologic function is not completely understood. Using a bilateral uterine artery ligation model to induce UPI in the rat, our laboratory has previously shown that juvenile male IUGR offspring at postnatal day (P) 21 have decreased myelin basic protein/neuronal nuclei ratio in all subregions of the hippocampus (CA1, CA3, and dentate gyrus, DG) (5). In contrast, neurons and synaptic density were preserved at P21. This study aimed to determine the effects of UPI on hippocampal neuronal, astrocytic, and immature oligodendrocytic composition at birth (P0) to determine whether IUGR offspring are born with a different cellular composition that then changes as the offspring matures.

A second aim of this study was to determine how UPI affects neural stem cells (NSCs), the progenitor cells that give rise to neurons and glia, when UPI is occurring. In particular, we will examine how UPI affects the molecules that govern NSC differentiation into neurons and glia. These molecules include the ErbB receptors (ErbB-Rs) and their ligand, neuregulin 1 (NRG1). The ErbB-R family includes ErbB2, ErbB3, and ErbB4. Once ErbB3 and ErbB4 bind to NRG1, they must heterodimerize with ErbB2 for cell fate regulation (6,7). ErbB2 has no known endogenous ligand.

We therefore hypothesized that IUGR rat hippocampi would have decreased numbers of neurons, astrocytes, and immature oligodendrocytes at P0, with males showing greater cellular deficits. We further hypothesized that UPI would perturb rat hippocampal expression of ErbB-Rs and NRG1 at P0 and P21 to account for the short- and long-term cellular changes of IUGR. To test these hypotheses, we employed our rat model of bilateral uterine artery ligation to induce UPI, producing asymmetrical IUGR pups born 20–25% lighter in weight but with demonstrable cerebral alterations (8–11). We focused on the hippocampus in this study because this structure is intimately involved in learning and memory, is particularly susceptible to metabolic disturbances such as UPI (1,12), and harbors a NSC niche within the DG (13).

The first two authors contributed equally to this study.

<sup>1</sup>Department of Pediatrics, University of Utah School of Medicine, Salt Lake City, Utah. Correspondence: Camille Fung ([camille.fung@hsc.utah.edu](mailto:camille.fung@hsc.utah.edu))

Received 11 October 2011; accepted 2 February 2012; advance online publication 4 April 2012. doi:10.1038/pr.2012.32

## RESULTS

**Dorsal Hippocampal Subregional Volumes in Control and IUGR Animals at P0**

IUGR significantly decreased female DG volume at P0 as compared with control (CON) females (Figure 1). IUGR, on the other hand, significantly decreased CA1 volume in males at P0 as compared with CON males (Figure 1). CON female and CON male hippocampal subregional volumes were similar (Figure 1).

**Hippocampal Neurons, Astrocytes, and Immature Oligodendrocytes in CON and IUGR Animals at P0**

In the DG, CON males had a baseline decrease in neuron number as compared with CON females (Figure 2a). IUGR decreased neuron number in the DG in females only (Figures 2a and 3a). In contrast, IUGR decreased the number of neurons in the CA3 and CA1 regions in males only (Figures 2b,c and 3b,c).

As with DG neurons, CON males had a baseline decrease in the number of astrocytes as compared with CON females (Figure 4a). IUGR increased the number of DG astrocytes in males only (Figures 3d and 4a). On the other hand, IUGR decreased the number of CA3 astrocytes in males only (Figures 3e and 4b). IUGR did not significantly affect the number of CA1 astrocytes in either gender (Figure 4).

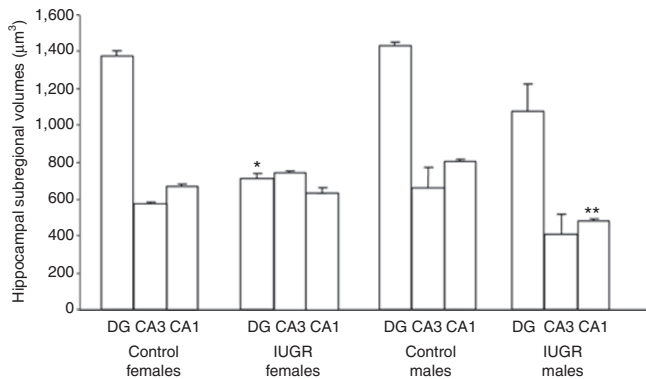


**Figure 1.** Quantification of dorsal hippocampal DG, CA3, and CA1 subregional volumes at postnatal day 0. Hippocampal subregional volumes are depicted as means  $\pm$  SEM in  $\mu\text{m}^3$ .  $n = 6/\text{group}$ . \* $P < 0.05$  vs. control females DG, \*\* $P < 0.05$  vs. control males CA1. DG, dentate gyrus; IUGR, intrauterine growth restriction.

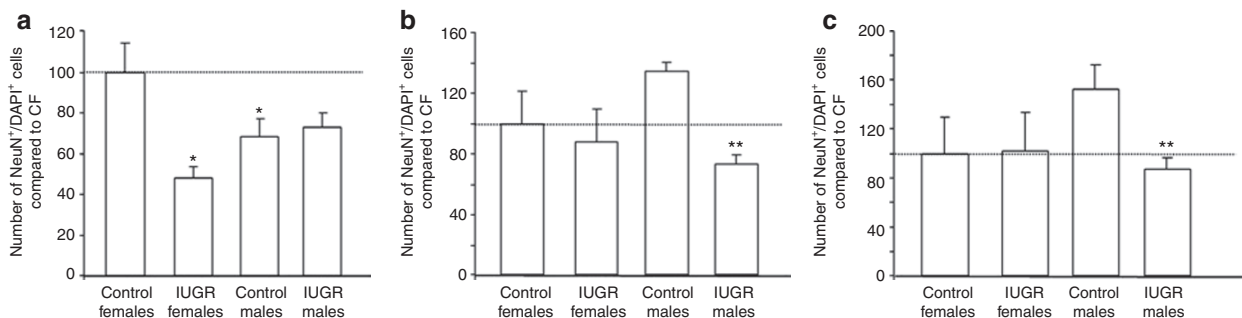


**Figure 2.** Quantification of neuron number in CON and IUGR hippocampal subregions at postnatal day 0. Quantification of neuron number in hippocampal (a) DG, (b) CA3, and (c) CA1. Data are normalized to control females (CF) set at 100%. \* $P < 0.05$  vs. control females, \*\* $P < 0.05$  vs. control males. DAPI, 4',6-diamidino-2-phenylindole; DG, dentate gyrus; NeuN, neurons with neuronal nuclear antigen; IUGR, intrauterine growth restriction.

Finally, IUGR did not significantly alter the number of immature oligodendrocytes in DG or CA3 in either gender (Figure 5 a,b). IUGR significantly increased the number of CA1 immature oligodendrocytes in females (Figure 3f and 5c) but decreased the number of CA1 immature oligodendrocytes in males (Figure 5c).

**Hippocampal ErbB2 Protein Levels at P0 and P21**

IUGR females at P0 had increased hippocampal ErbB2 protein levels as compared with CON females (Figure 6). On the other hand, IUGR males at P0 had similar ErbB2 protein levels to those of CON males. CON females and males had similar ErbB2 protein levels at baseline. At P21, CON males had an increased baseline ErbB2 protein level as compared with CON females (Figure 6). IUGR did not alter ErbB2 protein levels in either gender at this age (Figure 6).

**Hippocampal ErbB3 Protein Levels at P0 and P21**

IUGR males and females at P0 had decreased ErbB3 protein levels as compared with gender-matched CONs (Figure 6). CON females and males had similar ErbB3 protein levels at baseline. At P21, CON males had increased baseline ErbB3 protein levels relative to CON females, similar to that seen with ErbB2 protein expression (Figure 6). IUGR males showed a further increase in ErbB3 protein levels relative to CON males.

**Hippocampal ErbB4 Protein Levels at P0 and P21**

At P0, CON males showed an increased baseline ErbB4 protein level relative to CON females. IUGR did not alter ErbB4 protein levels in either gender at P0 (Figure 7). IUGR also did not affect ErbB4 protein levels in either gender at P21 (Figure 7).

**Hippocampal NRG1 Protein Levels at P0 and P21**

At P0 and P21, IUGR females and males had similar hippocampal NRG1 protein levels as their age- and gender-matched CONs (Figure 7). In addition, CON males at P21 had an increased NRG1 protein level as compared with CON females (Figure 7).

## DISCUSSION

The most important finding of this study is that an acute UPI insult alters hippocampal neuronal, astrocytic, and immature

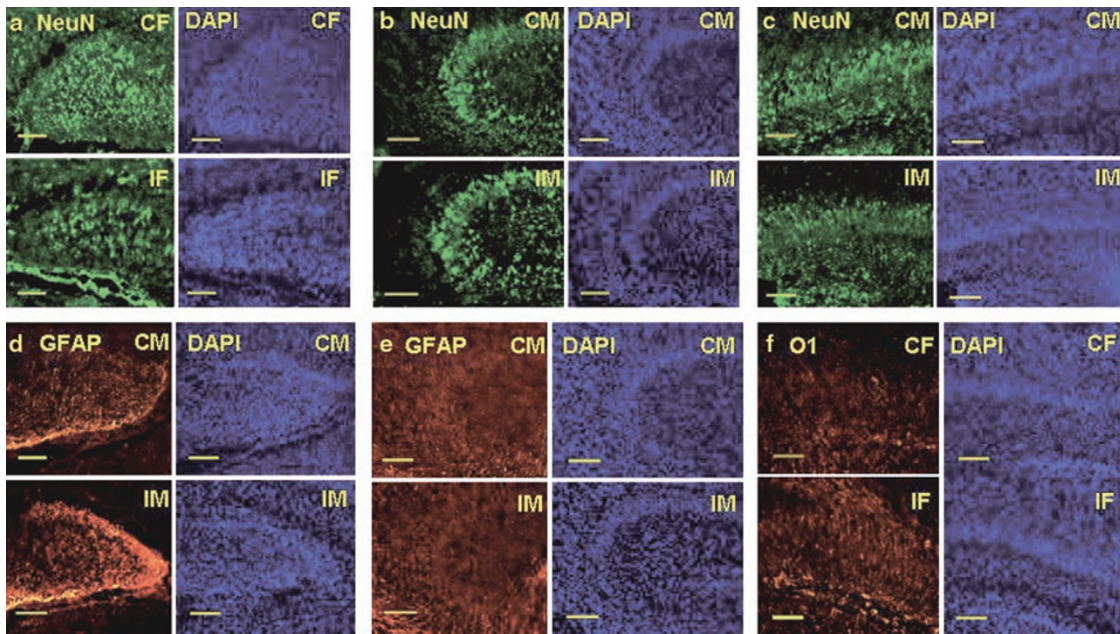


**Figure 3.** NeuN, GFAP, and O1 immunofluorescent staining for neurons, astrocytes, and immature oligodendrocytes, respectively, in CON and IUGR hippocampal DG, CA3, and CA1 subregions at postnatal day 0. Representative hippocampal NeuN and DAPI immunofluorescent microscopic images from (a) DG of control females (CF) and IUGR females (IF), and from (b) CA3 and (c) CA1 of control males (CM) and IUGR males (IM). Representative hippocampal GFAP and DAPI immunofluorescent microscopic images from (d) DG and (e) CA3 of CM and IM. Representative hippocampal O1 and DAPI immunofluorescent microscopic images from (f) CA1 of CF and IF. *n* = 6/group. Bars = 50  $\mu$ m. DAPI, 4',6'-diamidino-2-phenylindole; DG, dentate gyrus; GFAP, glial fibrillary acidic protein; NeuN, neurons with neuronal nuclear antigen; IUGR, intrauterine growth restriction.

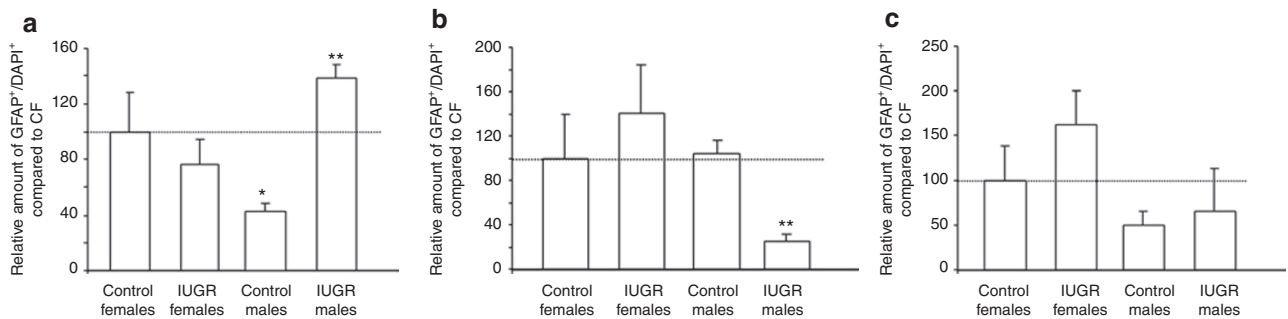


**Figure 4.** Quantification of relative numbers of astrocytes in control and IUGR hippocampal subregions at postnatal day 0. Quantification of relative numbers of astrocytes in hippocampal (a) DG, (b) CA3, and (c) CA1. Data are normalized to control females (CF) set at 100%. \**P* < 0.05 vs. control females, \*\**P* < 0.05 vs. control males. DAPI, 4',6'-diamidino-2-phenylindole; DG, dentate gyrus; GFAP, glial fibrillary acidic protein; IUGR, intrauterine growth restriction.

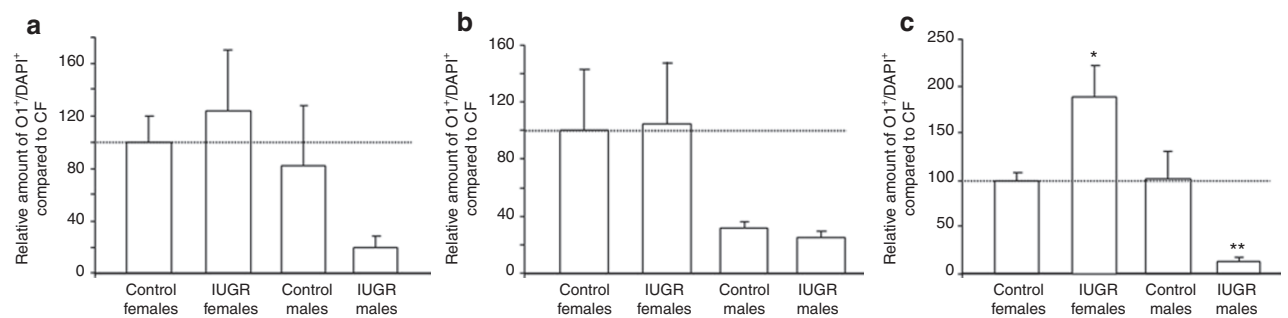


**Figure 5.** Quantification of relative numbers of immature oligodendrocytes in control and IUGR hippocampal subregions at postnatal day 0. Quantification of relative numbers of immature oligodendrocytes in hippocampal (a) DG, (b) CA3, (c) and CA1. Data are normalized to control females (CF) set at 100%. \**P* < 0.05 vs. control females, \*\**P* < 0.05 vs. control males. DAPI, 4',6'-diamidino-2-phenylindole; DG, dentate gyrus; IUGR, intrauterine growth restriction.



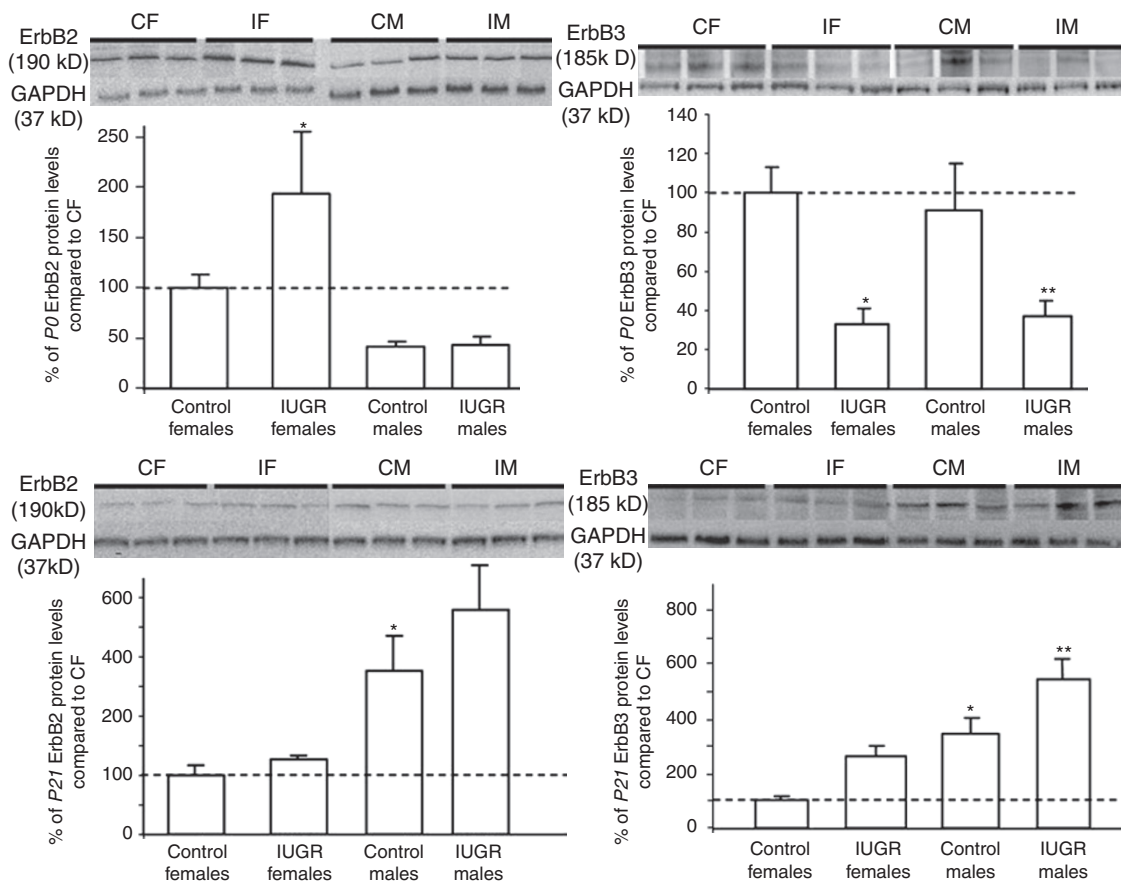


**Figure 6.** Quantification of hippocampal ErbB2 and ErbB3 protein levels at postnatal day (P) 0 and P21. Results are depicted as % means  $\pm$  SEM as compared with control females set as 100% ( $n = 6/\text{group}/\text{time point}$ ). Representative western blots are depicted above the western quantification. Glyceraldehyde-3-phosphate dehydrogenase (GAPDH) acted as loading control. \* $P < 0.05$  vs. control females, \*\* $P < 0.05$  vs. control males. CF, control females; CM, control males; IF, IUGR females; IM, IUGR males; IUGR, intrauterine growth restriction.

oligodendrocytic composition in the rat IUGR offspring at birth in a region- and gender-specific manner. Along with altered hippocampal cellular composition, ErbB receptor expression is also altered in a receptor- and gender-specific manner. Collectively, these data provide a link to how the altered IUGR hippocampal cellular phenotype may result from altered NSC differentiation molecules such as the ErbB-R.

In our model, IUGR rat offspring showed a decrease in hippocampal neuron number at birth. This neuronal decrease is consistent with neuronal decreases observed in other animals that have undergone UPI (14,15). However, important differences in our findings as compared with these studies are in the region- and gender-specificity of these neuronal changes. Whereas other models have shown decreased number of neurons within one brain region only, i.e., in the cerebral cortex or hippocampal CA1, our investigation separated the three main subregions of the hippocampus to highlight regional differences. In addition, we separated our analyses based on gender in an attempt to understand whether being an IUGR male or female would portend different outcomes. What we found was that IUGR males had decreased hippocampal CA1 and CA3 neurons, whereas IUGR females had decreased DG neurons.

Possible explanations for such region- and gender-specific neuronal decreases are multiple. CA1 and CA3 neurons arise separately by location and timing from the DG neurons during embryonic life. CA1 and CA3 neurons, which originate from the ammonic neuroepithelium, are produced mostly during embryonic day 17 (E17) to E20 in the rat brain. DG neurons, which originate from the dentate neuroepithelium, are produced mostly during E18 to E22 (16,17). The molecular control governing these morphogenetic events is also known to be region-specific (18). In addition, neurons in hippocampal subregions possess different intrinsic vulnerability to injury. A recent study demonstrated that prenatal stress in pregnant rats elicited increased spine density on CA1 pyramidal neurons in male pups only (19). Furthermore, prenatal stress altered DG granular neuron spine density, dendritic length, and complexity in opposite directions in male and female offspring. Together, neurons from different brain regions and from different genders will behave differently in response to an insult because of their inherent regional and sex-autonomous differences.

Another explanation for our observed region- and gender-specificity may relate to the fact that neurons in IUGR male hippocampi are exposed to an environment of testosterone-estradiol imbalance. We have previously shown that our IUGR

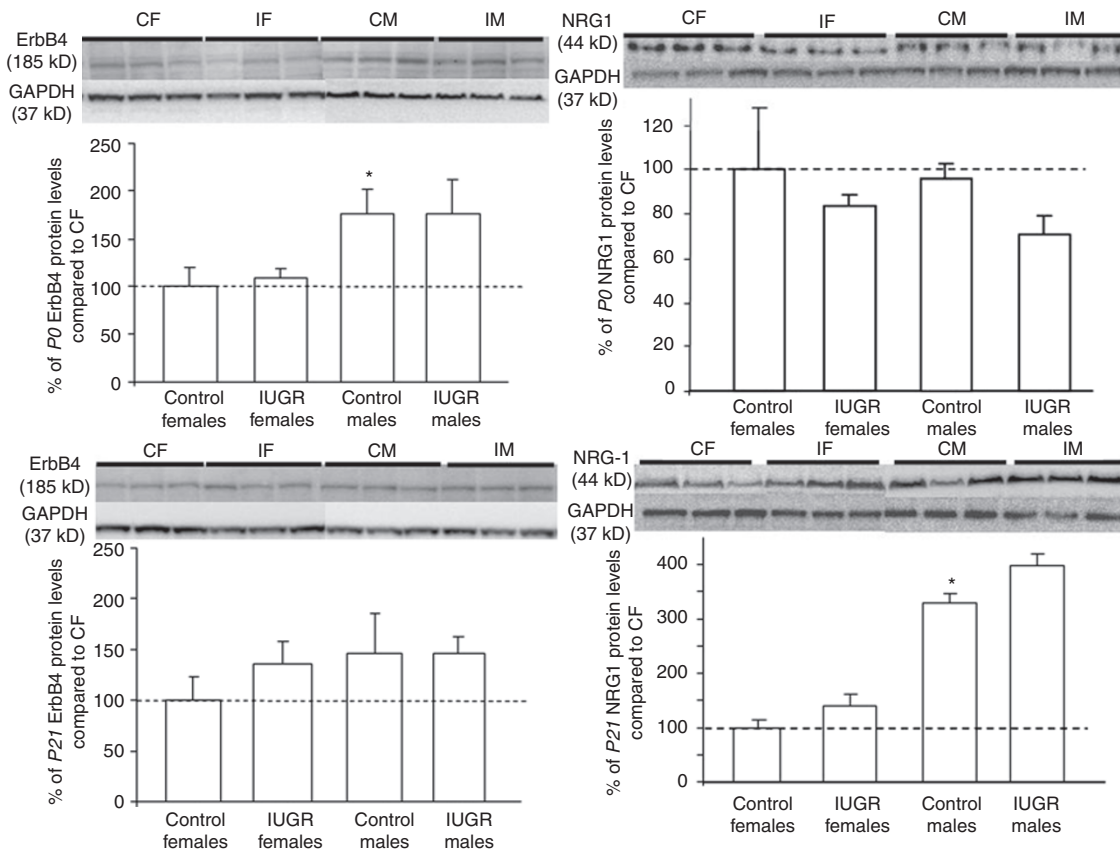


**Figure 7.** Quantification of hippocampal ErbB4 and neuregulin 1 (NRG1) protein levels at postnatal day (P) 0 and P21. Results are depicted as % means  $\pm$  SEM as compared with control females set as 100% ( $n = 6/\text{group}/\text{time point}$ ). Representative western blots are depicted above the western quantification. Glyceraldehyde-3-phosphate dehydrogenase (GAPDH) acted as loading control. \* $P < 0.05$  vs. control females. CF, control females; CM, control males; IF, IUGR females; IM, IUGR males; IUGR, intrauterine growth restriction.

males at birth have increased serum testosterone level in association with decreased hippocampal aromatase expression whereas IUGR females do not (20). Aromatase is the enzyme responsible for the conversion of testosterone to its metabolite estradiol. The exposure of the developing brain to a balanced testosterone and estradiol ratio is critical for proper neuronal development (21). Therefore, overexposure of the earlier-formed CA1 and CA3 neurons to an excess of testosterone in our IUGR male rats may account for the selective regional neuronal loss.

In addition to neuronal decreases, UPI elicited region- and gender-specific astrocytic and immature oligodendrocytic changes at birth. Important to highlight here is that unlike the situation with respect to neurons, IUGR males possessed opposing numbers of astrocytes in DG and CA3 regions of the rat hippocampus as compared with control males. Opposing astrocytic numbers in other chronic insults of UPI have been demonstrated in the cortices of guinea pigs and rabbits (22,23). But opposing astrocytic numbers within subregions of one brain structure have not been seen previously. The etiology of these astrocytic differences remains unclear. We speculate that some of our explanations pertaining to the subregional neuronal differences may account for the subregional differences observed in astrocytes as well.

In terms of our findings with immature oligodendrocytes, UPI in this model produced a strong gender difference in the hippocampal CA1 region. Of importance is that IUGR males had decreased numbers of immature oligodendrocytes at birth. As seen in our previous work, IUGR males had decreased myelin basic protein/neuronal nuclei ratio in the same region at P21 (5). The current finding adds to the previous result by suggesting that the reduction in CA1 oligodendrocytic precursors at birth reduced the capacity to generate mature myelin basic protein at P21. Such an overall reduction in CA1 myelin basic protein will negatively affect the hippocampal function of IUGR males in the long term, as CA1 neurons are responsible for sending the main hippocampal output back to the cortex for information processing (24).

The region- and gender-specific neuronal and glial changes observed in our model suggest that NSC differentiation is altered by UPI. ErbB receptors and their ligand, NRG1, are known to play critical roles in neuronal and glial development from NSCs (6,25). Mice deficient in ErbB2, 3, or 4 receptor have all died at relatively early stages of development, making a complete analysis of the central nervous system phenotype difficult. ErbB2-null mice show marked abnormalities of their cranial ganglia (26), whereas ErbB4-null mice have abnormal innervation of the

brainstem (27). Furthermore, ErbB receptors are known to be localized in NSCs of both rodents and humans (28–30). Within the germinal epithelia of the developing Sprague-Dawley rat brain, ErbB2 and ErbB4 mRNAs have been found to be widely distributed as early as E12 (28). As rat brain development progressed, ErbB2 mRNA was mainly confined to the cells of the ventricular zone, whereas ErbB4 mRNA was mainly localized to the cells of the subventricular zone. These zones represent NSC niches in the developing and adult brain.

In our current study, IUGR females at birth had decreased amounts of hippocampal ErbB3 receptor despite no change in NRG1 ligand expression. Hippocampal ErbB3 receptor decrease occurs in conjunction with ErbB2 receptor increase. Because ErbB3 receptor lacks intrinsic kinase activity and must heterodimerize with ErbB2 for downstream signaling (31), the increase in ErbB2 receptor may signify a compensatory response to the IUGR decrease in ErbB3 levels. Of note, IUGR males also showed decreased amounts of hippocampal ErbB3 receptor at birth, but they lacked the ErbB2 receptor upregulation. Such a lack of ErbB2 receptor compensation may suggest that IUGR males are more susceptible to aberrant hippocampal morphogenesis because of their inability to transmit extracellular NRG1 signal for proper hippocampal NSC differentiation. This speculation is in part supported by the ErbB3 mutant mice who have a misshaped cerebellar plate that is poorly differentiated and contains fewer Purkinje cells as compared with the wild type (32).

We understand that limitations to our study exist. We have examined only total NRG1 expression. NRG1 has at least 15 known isoforms arising from alternative promoter usage and RNA splicing; therefore other NRG1 isoforms may be altered as a result of UPI. Another limitation is the mixed population of NSCs, neurons, and glia within the rat hippocampus. Ideally, isolating NSCs from the hippocampus would generate a more cell type-specific NRG1 and ErbB receptor expression profile. Future studies using NSC-specific nestin-green fluorescent protein transgenic mice will help to isolate a pure population of NSCs to elucidate the NSC-specific changes in ErbB receptor and NRG1.

In conclusion, our study has delineated for the first time the natal hippocampal neuronal and glial phenotype in a model of UPI that has been in use since the 1960s. Given the current recognition of how many adult-onset neurocognitive and neuropsychiatric disorders may have origins in fetal life (33,34), an understanding of how UPI affects the cellular makeup at birth and over time will open up mechanistic questions to address aberrant neural function in these IUGR offspring.

## METHODS

The University of Utah Animal Care Committee approved all procedures, which were carried out in accordance with the National Institute of Health Guide for the Care and Use of Laboratory Animals. The rat model of UPI has been previously described (5,35).

### Animal Perfusion for Histology

P0 pups ( $n = 6$ /group from three separate CON and three separate IUGR litters) were individually fixed via intracardiac perfusion with ice-cold 0.9% normal saline (vWR, Radnor, PA), followed by ice-cold 2% paraformaldehyde (Electron Microscopy Sciences, Hatfield,

PA)/1.4% sodium cacodylate (Sigma-Aldrich, St. Louis, MO)/5% sucrose (vWR) for 10 min. Dissected whole brains were postfixed at 4°C overnight, cryoprotected with 15% and 30% sucrose at 4°C overnight, and embedded in 2% gelatin, 0.9% NaCl, 0.05% Na<sub>2</sub>S<sub>2</sub>O<sub>8</sub> (Sigma-Aldrich) under freezing conditions. They were sectioned coronally with a cryostat at 10 μm per section (Microm HM550; Microm International, Walldorf, Germany). Sections were collected sequentially on 10 consecutive Superfrost Plus slides (Fisher Scientific, Pittsburgh, PA) such that the first and every tenth section were on the same slide.

### Nissl Stain to Quantify Dorsal Hippocampal Subregional Volumes at P0

Sections encompassing the dorsal hippocampus were soaked in decreasing ethanol (vWR) baths. After two brief deionized H<sub>2</sub>O (DH<sub>2</sub>O) washes, sections were incubated in cresyl violet stain (Sigma-Aldrich) (1.25 g cresyl violet acetate and 0.75 ml glacial acetic acid to 250 ml warm DH<sub>2</sub>O) for 2 min and washed in DH<sub>2</sub>O for 1 min. Sections were dehydrated by a series of increasing ethanol baths and finally cleared by HistoClear (AGTC Bioproducts, Wilmington, MA) for 5 min. Sections were covered with mounting medium, coverslipped, and examined under light microscopy at ×15 and ×30 magnifications.

### Morphometric Analyses of Nissl-Stained Dorsal Hippocampi at P0

Hippocampal DG, CA3, and CA1 subregions of the CON and IUGR groups at ×30 magnification were outlined manually using National Institutes of Health ImageJ software. Hippocampal subregional areas were calculated as a percentage of total hippocampal area. As each section was 10 μm thick, we calculated each subregion's volume according to the Cavalieri principle:  $V = \Sigma A \times P \times t$ , where  $V$  = total volume,  $\Sigma A$  = sum of measured areas,  $P$  = inverse of section sampling fraction, and  $t$  is section thickness (36). DG, CA3, and CA1 subregional volumes were generated for the CON and IUGR groups.

### Immunofluorescent Labeling of Neurons With Neuronal Nuclear Antigen (NeuN), of Astrocytes With Glial Fibrillary Acidic Protein (GFAP), and of Immature Oligodendrocytes With O1 at P0

Sections were blocked with 3% normal goat serum/0.05% Triton X-100 (Sigma-Aldrich) for 1 h at room temperature, incubated with mouse IgG monoclonal anti-NeuN antibody (MAB377; Millipore, Billerica, MA) at 1:1,000, rabbit polyclonal anti-GFAP antibody (ab7779; Abcam, Cambridge, MA) at 1:2,000, or mouse IgM monoclonal anti-immature oligodendrocyte marker O1 antibody (MAB1327; R&D systems, Minneapolis, MN) at 1:2,000 in 3% normal goat serum/0.05% Triton X-100 overnight at 4°C. Sections were washed three times in phosphate-buffered saline (Sigma-Aldrich) for 10 min and exposed to either secondary fluorescence-labeled DyLight™ 488-conjugated AffiniPure goat anti-mouse IgG at 1:1,000, Cy-3-conjugated goat anti-rabbit at 1:1,000, or DyLight™ 549-conjugated AffiniPure goat anti-mouse IgM at 1:2,000 (Jackson ImmunoResearch, West Grove, PA) in 3% normal goat serum/0.05% Triton X-100 for 1 h at room temperature. Cell nuclei were counterstained with 10 ng/ml 4',6-diamidino-2-phenylindole (DAPI) (Molecular Probes, Invitrogen, Eugene, OR). Sections were washed again three times in , air-dried, and coverslipped using Fluoromount-G mounting medium (Southern Biotech, Birmingham, AL). Negative control sections underwent similar staining procedure except for primary antibodies. Sections were imaged with the Olympus Fluoview FV1000 multiphoton laser scanning confocal microscope (Olympus Imaging America, Center Valley, PA) and taken at ×10 and ×20 magnification to encompass all subregions of the hippocampus (DG, CA3, and CA1).

### Morphometric Analyses of Immunofluorescent Staining at P0

Sections encompassing the dorsal hippocampi at Bregma level ~–3.0 according to (37) were used for quantification. The numbers of NeuN positive (NeuN<sup>+</sup>) neurons in DG, CA3, and CA1 were counted in the context of total DAPI<sup>+</sup> cells using National Institutes of Health ImageJ software. Because of subregional hippocampal volume differences, DAPI count was normalized to the subregion with the fewest cells.



Because GFAP and O1 largely stain for cell processes, we quantified the relative number of astrocytes or immature oligodendrocytes by GFAP<sup>+</sup> or O1<sup>+</sup> staining divided by normalized DAPI<sup>+</sup> cell nuclei.

#### Western Immunoblotting for ErbB-Rs and NRG1 at P0 and P21

Hippocampi were homogenized in ice-cold radioimmunoprecipitation assay buffer ( $n = 6$ /group with pups from three separate CON and three separate IUGR litters for each time point). Total protein concentration was determined by BCA Protein Assay (Pierce Biotechnology, Rockford, IL) using bovine serum albumin (Sigma-Aldrich) as a standard; 100  $\mu$ g of protein and molecular weight markers were separated by XT Criterion gel electrophoresis (Bio-Rad Laboratories, Hercules, CA) at 200 V for 1 h. After electrophoresis, proteins were transferred to polyvinylidene fluoride membranes (Millipore) overnight at 4°C. Post-transfer, membranes were blocked in 5% milk/Tris-buffered saline Tween (TBS-T) at room temperature for 1–1.5 h. Bound proteins were detected with antibodies against ErbB2 (ab2428, Abcam) 1:200 in 5% milk/TBS-T; ErbB3 (05-390, Millipore) 1:100 in 5% milk/TBS-T; ErbB4 (ab19391, Abcam) 1:100 in 5% milk/TBS-T; total NRG1 (ab2994, Abcam) 1:150 in 5% milk/TBS-T; glyceraldehyde-3-phosphate dehydrogenase (GAPDH) (2118; Cell Signaling Technology, Danvers, MA) 1:2,000 in 5% milk/TBS-T at 4°C overnight. Membranes were probed with either horseradish peroxidase-conjugated anti-rabbit or anti-mouse IgG antibody at 1:2,000–1:3,000 in 5% milk (Cell Signaling) secondary antibody for 1 h at room temperature. Antibody signals were detected with Western Lighting enhanced chemiluminescence (PerkinElmer, Waltham, MA) and quantified with Kodak Image Station 2000R (Eastman Kodak/SIS, Rochester, NY). GAPDH served as the loading control. Hippocampal GAPDH protein expression was determined to be unaltered in our IUGR model (data not shown).

#### Statistics

Immunofluorescent histochemical quantification of NeuN, GFAP, and O1, normalized to CON females to highlight gender differences, is expressed as absolute values in arbitrary units. Protein levels of ErbB receptors and NRG1 are expressed as means  $\pm$  SEM, which were also normalized to CON females. Data were analyzed with ANOVA using Tukey *post hoc* test for equal sample sizes. Statistical significance was declared at  $P < 0.05$ .

#### ACKNOWLEDGMENTS

We thank Scott Rogers and Lorise Gahring for their expertise and guidance in immunofluorescent histochemistry and Christopher Rodesch for his expertise in immunofluorescent histochemical quantification.

#### STATEMENT OF FINANCIAL SUPPORT

This research was supported by National Institute of Child Health and Human Development Grant R01-HD-41075 (to R.H.L.) and University of Utah Children's Health Research Career Development Award 5K12-HD001410-06 (to C.F.).

#### REFERENCES

- van Wassenaer A. Neurodevelopmental consequences of being born SGA. *Pediatr Endocrinol Rev* 2005;2:372–7.
- Tolsa CB, Zimine S, Warfield SK, et al. Early alteration of structural and functional brain development in premature infants born with intrauterine growth restriction. *Pediatr Res* 2004;56:132–8.
- Jarvis S, Glinianaia SV, Torrioli MG, et al.; Surveillance of Cerebral Palsy in Europe (SCPE) collaboration of European Cerebral Palsy Registers. Cerebral palsy and intrauterine growth in single births: European collaborative study. *Lancet* 2003;362:1106–11.
- Lahti J, Rääkkönen K, Kajantie E, et al. Small body size at birth and behavioural symptoms of ADHD in children aged five to six years. *J Child Psychol Psychiatry* 2006;47:1167–74.
- Schober ME, McKnight RA, Yu X, Callaway CW, Ke X, Lane RH. Intrauterine growth restriction due to uteroplacental insufficiency decreased white matter and altered NMDAR subunit composition in juvenile rat hippocampi. *Am J Physiol Regul Integr Comp Physiol* 2009;296:R681–92.
- Buonanno A, Fischbach GD. Neuregulin and ErbB receptor signaling pathways in the nervous system. *Curr Opin Neurobiol* 2001;11:287–96.
- Shah NM, Marchionni MA, Isaacs I, Stroobant P, Anderson DJ. Glial growth factor restricts mammalian neural crest stem cells to a glial fate. *Cell* 1994;77:349–60.
- Lane RH, Kelley DE, Gruetzmacher EM, Devaskar SU. Uteroplacental insufficiency alters hepatic fatty acid-metabolizing enzymes in juvenile and adult rats. *Am J Physiol Regul Integr Comp Physiol* 2001;280:R183–90.
- Ke X, McKnight RA, Wang ZM, et al. Nonresponsiveness of cerebral p53-MDM2 functional circuit in newborn rat pups rendered IUGR via uteroplacental insufficiency. *Am J Physiol Regul Integr Comp Physiol* 2005;288:R1038–45.
- Ke X, Lei Q, James SJ, et al. Uteroplacental insufficiency affects epigenetic determinants of chromatin structure in brains of neonatal and juvenile IUGR rats. *Physiol Genomics* 2006;25:16–28.
- Lane RH, Ramirez RJ, Tsirka AE, et al. Uteroplacental insufficiency lowers the threshold towards hypoxia-induced cerebral apoptosis in growth-retarded fetal rats. *Brain Res* 2001;895:186–93.
- Lodygensky GA, Seghier ML, Warfield SK, et al. Intrauterine growth restriction affects the preterm infant's hippocampus. *Pediatr Res* 2008;63:438–43.
- Parent JM. Injury-induced neurogenesis in the adult mammalian brain. *Neuroscientist* 2003;9:261–72.
- Tashima L, Nakata M, Anno K, Sugino N, Kato H. Prenatal influence of ischemia-hypoxia-induced intrauterine growth retardation on brain development and behavioral activity in rats. *Biol Neonate* 2001;80:81–7.
- Mallard C, Loeliger M, Copolov D, Rees S. Reduced number of neurons in the hippocampus and the cerebellum in the postnatal guinea-pig following intrauterine growth-restriction. *Neuroscience* 2000;100:327–33.
- Altman J, Bayer SA. Mosaic organization of the hippocampal neuroepithelium and the multiple germinal sources of dentate granule cells. *J Comp Neurol* 1990;301:325–42.
- Altman J, Bayer SA. Migration and distribution of two populations of hippocampal granule cell precursors during the perinatal and postnatal periods. *J Comp Neurol* 1990;301:365–81.
- Li G, Pleasure SJ. Genetic regulation of dentate gyrus morphogenesis. *Prog Brain Res* 2007;163:143–52.
- Bock J, Murmu MS, Biala Y, Weinstock M, Braun K. Prenatal stress and neonatal handling induce sex-specific changes in dendritic complexity and dendritic spine density in hippocampal subregions of prepubertal rats. *Neuroscience* 2011;193:34–43.
- O'Grady SP, Caprau D, Ke XR, et al. Intrauterine growth restriction alters hippocampal expression and chromatin structure of Cyp19a1 variants. *Syst Biol Reprod Med* 2010;56:292–302.
- Schwarz JM, McCarthy MM. Steroid-induced sexual differentiation of the developing brain: multiple pathways, one goal. *J Neurochem* 2008;105:1561–72.
- Nitsos I, Rees S. The effects of intrauterine growth retardation on the development of neuroglia in fetal guinea pigs. An immunohistochemical and an ultrastructural study. *Int J Dev Neurosci* 1990;8:233–44.
- Bassan H, Kidron D, Bassan M, et al. The effects of vascular intrauterine growth retardation on cortical astrocytes. *J Matern Fetal Neonatal Med* 2010;23:595–600.
- Kealy J, Commins S. The rat perirhinal cortex: A review of anatomy, physiology, plasticity, and function. *Prog Neurobiol* 2011;93:522–48.
- Yarden Y, Sliwkowski MX. Untangling the ErbB signalling network. *Nat Rev Mol Cell Biol* 2001;2:127–37.
- Lee KF, Simon H, Chen H, Bates B, Hung MC, Hauser C. Requirement for neuregulin receptor erbB2 in neural and cardiac development. *Nature* 1995;378:394–8.
- Gassmann M, Casagrande F, Orioli D, et al. Aberrant neural and cardiac development in mice lacking the ErbB4 neuregulin receptor. *Nature* 1995;378:390–4.
- Kornblum HI, Yanni DS, Easterday MC, Seroogy KB. Expression of the EGF receptor family members ErbB2, ErbB3, and ErbB4 in germinal zones of the developing brain and in neurosphere cultures containing CNS stem cells. *Dev Neurosci* 2000;22:16–24.
- Fox IJ, Kornblum HI. Developmental profile of ErbB receptors in murine central nervous system: implications for functional interactions. *J Neurosci Res* 2005;79:584–97.

30. Chong VZ, Webster MJ, Rothmond DA, Weickert CS. Specific developmental reductions in subventricular zone ErbB1 and ErbB4 mRNA in the human brain. *Int J Dev Neurosci* 2008;26:791–803.
31. Esper RM, Pankonin MS, Loeb JA. Neuregulins: versatile growth and differentiation factors in nervous system development and human disease. *Brain Res Rev* 2006;51:161–75.
32. Erickson SL, O’Shea KS, Ghaboosi N, et al. ErbB3 is required for normal cerebellar and cardiac development: a comparison with ErbB2- and heregulin-deficient mice. *Development* 1997;124:4999–5011.
33. Joss-Moore LA, Lane RH. The developmental origins of adult disease. *Curr Opin Pediatr* 2009;21:230–4.
34. Entringer S, Buss C, Wadhwa PD. Prenatal stress and developmental programming of human health and disease risk: concepts and integration of empirical findings. *Curr Opin Endocrinol Diabetes Obes* 2010;17:507–16.
35. Baserga M, Hale MA, Wang ZM, et al. Uteroplacental insufficiency alters nephrogenesis and downregulates cyclooxygenase-2 expression in a model of IUGR with adult-onset hypertension. *Am J Physiol Regul Integr Comp Physiol* 2007;292:R1943–55.
36. Gundersen HJ, Jensen EB. The efficiency of systematic sampling in stereology and its prediction. *J Microsc* 1987;147(Pt 3):229–63.
37. Paxinos G, Charles W. *The Rat Brain in Stereotaxic Coordinates*, 4th edn. San Diego: Academic Press, 1998.